JTTEE5 20:186–194
DOI: 10.1007/s11666-010-9566-0
1059-9630/$19.00 © ASM International

Design of Experiment Analysis of the Sulzer Metco DJ High Velocity Oxy-Fuel Coating of Hydroxyapatite for Orthopedic Applications

S. Hasan and J. Stokes

(Submitted April 28, 2010; in revised form September 15, 2010)

High Velocity Oxy-Fuel (HVOF) has the potential to produce hydroxyapatite (HA; Bio-ceramic) coatings based on its experience with other sprayed ceramic materials. This technique should offer mechanical and biological results comparable to other thermal spraying processes, such as atmospheric plasma thermal spray, currently FDA approved for HA deposition. Deposition of HA via HVOF is a new venture especially using the Sulzer Metco Diamond Jet (DJ) process, and the aim of this article was to establish this technique's potential in providing superior HA coating results compared to the FDA-approved plasma spray technique. In this research, a Design of Experiment (DOE) model was developed to optimize the Sulzer Metco DJ HVOF process for the deposition of HA. In order to select suitable ranges for the production of HA coatings, the parameters were first investigated. Five parameters (factors) were researched over two levels namely: oxygen flow rate, propylene flow rate, air flow rate, spray distance, and powder flow rate. Coating crystallinity and purity were measured at the surface of each sample as the responses to the factors used. The research showed that propylene, air flow rate, spray distance, and powder feed rate had the largest effect on the responses, and the study aimed to find the preferred optimized settings to achieve high crystallinity and purity of percentages of up to 95%. This research found crystallinity and purity values of 93.8 and 99.8%, respectively, for a set of HVOF parameters which showed improvement compared to the crystallinity and purity values of 87.6 and 99.4%, respectively, found using the FDA-approved Sulzer Metco Atmospheric Plasma thermal spray process. Hence, a new technique for HA deposition now exists using the DJ HVOF facility; however, other mechanical and biorelated properties must also be assessed.

Keywords design of experiments, femoral implants, HVOF, hydroxyapatite, plasma spray

1. Introduction

Of all the existing advanced coatings techniques, the High Velocity Oxy-Fuel (HVOF) is one of the most popular thermal spray technologies. The flexibility and superior quality of coating obtained by this technique have made it the excellent choice for many industries, compared with other thermal spraying techniques, though it is relatively a new thermal spray process (Ref 1). HVOF thermal spray process develops superior quality of coating compared with other thermal spray techniques, like plasma thermal spray which is one of the currently FDA approved methods to spray HA (Ref 2). There are many different thermal spray processes available for the deposition of materials, but the atmospheric plasma thermal spray (Ref 2, 3) and the Detonation-Gun Spraying (D-gun) (Ref 4-6) are the processes chosen to deposit HA. HA is a calcium phosphate bioactive material. Because of its excellent biocompatibility, bone-bonding ability (allowing bone cells to grow on its surface), and identical chemical composition which is similar to the mineral phase of hand tissue in human bones, HA has been used in implant application for many years (Ref 2). The main objective of this research study is to investigate and optimize the HVOF spray parameters used while depositing HA onto surgical substrates. This was conducted using Design of Experiment (DOE) techniques to develop mathematical models. The developed models were useful in predicting responses like crystallinity and purity. It was hypothesized that for the first time Sulzer METCO Diamond Jet (DJ) HVOF may achieve higher crystallinity and purity than those of the FDA-approved plasma spray process.

This article is an invited paper selected from presentations at the 2010 International Thermal Spray Conference and has been expanded from the original presentation. It is simultaneously published in *Thermal Spray: Global Solutions for Future Applications, Proceedings of the 2010 International Thermal Spray Conference*, Singapore, May 3-5, 2010, Basil R. Marple, Arvind Agarwal, Margaret M. Hyland, Yuk-Chiu Lau, Chang-Jiu Li, Rogerio S. Lima, and Ghislain Montavon, Ed., ASM International, Materials Park, OH, 2011.

S. Hasan and **J. Stokes**, Materials Processing Research Centre & National Centre For Plasma Science and Technology, Dublin City University, Dublin, Ireland. Contact e-mail: joseph.t.stokes@dcu.ie.

2. Hydroxyapatite

Hydroxyapatite (HA) is a hydrated calcium phosphate mineral. The chemical formula of HA is $Ca_{10}(PO_4)_6(OH)_2$, and it has Ca/P ratio of 1.67 (Ref 7). Calcium phosphate ceramics have been used for dental implants, periodontal treatment, alveolar ridge augmentation, orthopedics, maxillofacial surgery, and otolaryngology for approximately 30 years (Ref 8). They are used as a coating material applied onto tougher substrates because of their inherent brittleness in the case of loading bearing applications. For example, HA coatings and HA composite coatings are used commercially for hip and knee replacements (Ref 7). It was also observed that the amount of bone growth on an uncoated steam (Ref 9, 10) can be lower than the bone growth achieved on HA.

2.1 Hydroxyapatite Powder

The quality of any thermal spray coating depends on the shape and microstructure of the HA powder used for coating (Ref 7). In the case of flow properties, spherical particles are better than angular particles. More consistent coatings are possible if the particle size range distribution is narrow. The most important characteristics of HA powder is its composition and crystallinity. Ceramic HA for surgical implants should have a minimum HA content of 95% according to the ASTM Standard Specification (ASTM Designation: F1185-88; Ref 11). This HA content is determined by a quantitative x-ray diffraction analysis. The XRD pattern for the Plasma Biotal Captal 60-1 HA powder shown in Fig. 1 is used to measure the purity and crystallinity of the HA powder. The maximum allowable total limit of all the heavy metals is 50 ppm, and the Ca/P ratio for HA used for surgical implants must be between 1.65 and 1.82 (Ref 11). Figure 2 shows the micrograph of Plasma Biotal Captal 60-1 HA powder particles which were used to coat HA by the DJ HVOF thermal spraying facility. It is clear from the scanning electron micrograph (SEM) that the particles consist of a mixed collection of smaller and agglomerate particles, because of the Plasma Biotal powder production process used. In this research, the particle size of hydroxyapatite powder used was 45 μm (Ref 2). Mechanical properties within the coating vary if the powder is sintered or spray-dried (Ref 12). Amorphous and crystalline phases are present in all biomedical devices. According to Gross et al. (Ref 12), amorphous phases can have hardness values of 1.5 ± 0.3 GPa and crystalline phase of 3.0-7.7 GPa.

2.2 Coating Purity

The most important method for determining the atomic arrangements in matter is x-ray Diffraction (XRD). It is used to provide information on the physical state of the sample and also to identify the phases present in samples. Coating purity can be calculated using (Ref 2).

$$\text{Purity}\ (\%) = \frac{\sum A_c - \sum A_i}{\sum A_c} \times 100 \qquad \text{(Eq 1)}$$

where $\sum A_c$ = The sum of the areas of all HA crystalline peaks and $\sum A_i$ = The sum of the area of the impurity peaks.

According to the ISO standard specification (ISO 13779-2:2000; Ref 13), the maximum allowable level of other non-HA phases in plasma spray HA coating is 5%. The phase purity of HA coatings is important because of the differences in dissolution properties between the different calcium phosphate phases.

2.3 Coating Crystallinity

High crystallinity in a coating is derived mainly from the unmelted core of powder particles. The crystallinity of a HA coating depends on the degree of melting of the powder particles. For medical application, the required crystallinity is more than 95% (Ref 13). In general, the Crystallinity of HA plasma spray coating is about 65-70% for biomedical use (Ref 14). It may also vary with thickness through the deposit (Ref 12). The crystallinity of HA

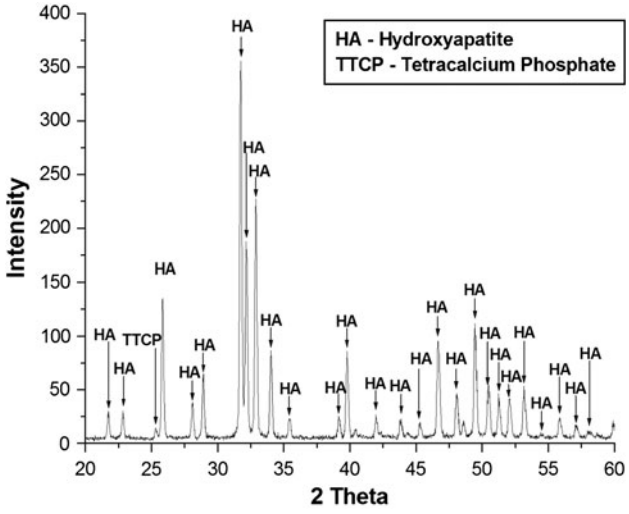

Fig. 1 Plasma Biotal Captal 60-1 HA powder XRD pattern

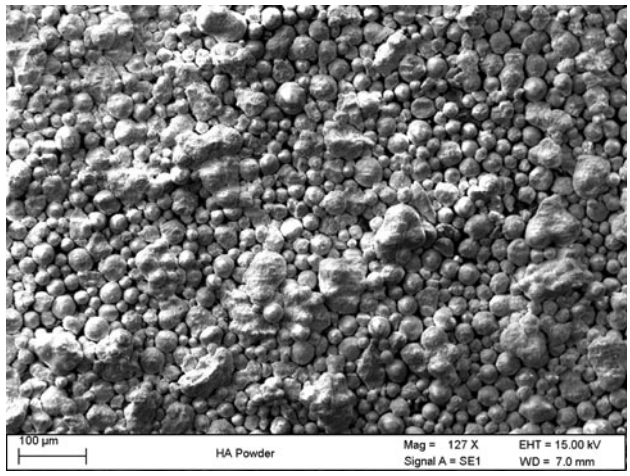

Fig. 2 Plasma Biotal Captal 60-1 HA powder micrograph

coating can be determined by various methods. The most commonly method for determining crystallinity is the Rutland Method (Ref 14-16). Crystallinity of HA coating can be calculated using (Ref 2).

$$\text{Crystallinity}\ (\%) = \frac{\sum A_c}{\sum A_c + \sum A_a} \times 100 \qquad \text{(Eq 2)}$$

where $\sum A_c$ = The sum of the areas of all HA crystalline peaks and $\sum A_a$ = The sum of the area under the amorphous peak.

3. Optimization of HA Coatings

3.1 Two-Level Factorial Experiment

A two-level full factorial experimental design uses all possible factor levels in determining its model. The Design Expert Design of Experiments (DOE) software by Stat-Ease© offers 2-21 factors for up to experimental 512 runs. Two levels may minimize the number of experiment tests, but the DOE must still give optimal results using the models it applies. For this research, a 2^5 experimental study was used to study five factors over two levels which consisted of 32 experiments.

3.2 Analysis of Variance (ANOVA)

DOE models can be assessed using Analysis Of Variance (ANOVA). The statistical significance of the models originated can be found out on the basis of a number of sufficiency measures like Adequate Precision R^2, Adjusted R^2, and Predicted R^2 are the most important. The aim is to achieve an adjusted and predicted R^2 to be as close to 1 in all, and to have a difference of 0.2 or less between them.

3.3 Optimizing HA Coatings

Higher quality HA coatings are always necessary. In view of this, it is very important to understand the scientific phenomena involved in their production. The classical experimental model adopted in the optimization of HA coatings is to vary one spray parameter at a time (Ref 17-20). Other researchers have statistically optimized their studies on plasma-sprayed coatings of various other materials, such as titanium nitride (Ref 21), alumina-titania (Ref 22, 23), alumina (Ref 24-26), and zirconia (Ref 27) using DOE techniques. Statistical experimentation of plasma-sprayed hydroxyapatite coatings was recently conducted by researchers, e.g., Cizek et al. (Ref 28) and Dyshlovenko et al. (Ref 29, 30).

3.4 Parameter Selection

A large number of parameters affect the HVOF thermal spray process. Parameters that are found to influence the coating properties should be selected for investigation using a screening experiment. One should select as many process parameters as possible, and only those which do not influence the coating properties can be omitted from further optimization investigations.

Table 1 Summary of DOE studies of HVOF-sprayed HA coatings

Experiment type	Description	Factors	Responses
2^5 factorial design	5 factors; 2 levels; 2 responses; 32 experiments	Oxygen flow meter reading; Propylene flow meter reading; Air flow meter reading; Spray distance; Powder feed rate	Crystallinity; Purity

Oxygen flow rate, propylene flow rate, air flow rate, spray distance, spray rate, powder, traverse velocity, deposition time, substrate roughness, gun nozzle, and substrate's pre-heat have all been found to have an influence on HVOF thermal spray coatings (Ref 31). Captal 60-1 thermal spray HA powder was used for all experimental studies; hence this was fixed, as this is also approved by the FDA for plasma spraying. The stand-off distance (SOD) or spray distance between the work piece and the spray gun can have a major influence. The velocity of droplets may decrease during spraying if the spray distance is large due to frictional forces from air molecules (Ref 15). Spray distance also affects the temperature of the work piece and thus coating deposition. An increase of spray distance causes coating properties to deteriorate as investigated by several researchers (Ref 15, 20, 32). The traverse speed chosen was the one that was optimized by Stokes (Ref 33), which was 200 mm/s, and the same was used, but this can also have an influence on coating buildup (Ref 34, 35). Deposition time for samples was not considered for further investigation because it only affects the thickness; therefore, the aim was to produce between 200- and 300-μm thickness using 10 passes of the gun, within the FDA-stipulated thickness requirement (Ref 2). A summary of the DOE studies investigated in this research is given in Table 1. In contrast to HVOF spraying, in plasma spray with argon gas, argon is often used as a powder carrier gas and primary plasma forming gas (Ref 2), whereas nitrogen is used as powder carrier gas in HVOF spraying research (Ref 31). Levingstone (Ref 2) used a traverse velocity of 38 mm/s which was held constant with a spray distance of 0-170 mm, powder feed rate of 20 g/min, and argon ionizing gas flow rate of 105 SLPM, and a current value of 750 A. In this research, current and gas flow rate and the interaction between them were found to have the major positive influence on crystallinity and purity, with spray distance and powder feed rate having secondary effects (Ref 2).

3.5 Parameter Level Selection

As a two-level factorial design was chosen, the maximum and minimum possible settings for each parameter are shown in Table 2. Feasible coatings were produced by varying each of the parameters. Whether or not a feasible coating was produced was determined visually identifying if a coating was deposited or not.

4. Results and Discussion

4.1 Coating Crystallinity and Purity

Coating crystallinity and purity of the Plasma Biotal HA-coated rectangular samples were found using the x-ray diffraction (XRD) technique. The XRD pattern for all the samples contained crystalline peaks showing traces of amorphous phase. The XRD pattern for sample 24 (the highest crystallinity coating) is shown in Fig. 3. The peaks in the pattern show that the main phases present were HA (JCPDS 9-0432), and a minor trace of tetracalcium phosphate (JCPDS 25-1137) was also present with insignificant phases of CaO and β-TCP. The XRD pattern for sample 29 (the lowest crystallinity coating) is shown in Fig. 4, where only the HA phase (JCPDS 9-0432) was present. However, a large amount of amorphous phase was detected, which supports findings by other authors (Ref 36, 37). The standard diffraction pattern for HA (JCPDS 9-0432) was compared with the peaks present in the diffraction patterns to the coating, which proved that the analyzed coating was HA. Coating crystallinity was found to vary for all the samples (from 93.81% in sample 24 to 74.94% in sample 29). According to ISO 13779-2:2000 (Ref 38), the minimum crystallinity required for Bio-HA coatings was 45%, but ideally the aim was to achieve results similar to plasma spraying which is FDA approved for clinical use, that is >90% crystallinity. Figure 5 shows the microstructure of sample 24. Porosity and a high degree of melting were observed using the parameters selected. The porosities found were similar to the thickness achieved around 30 μm, which is beneficial for cell ingress during femoral implantation. This porosity is high for HVOF systems but is more desirable for HA applications and similar to that achieved by APS techniques.

Table 2 Equipment limits for the selected spray parameters

Parameter	Minimum	Maximum
Oxygen flow meter reading		
(FMR)	30	45
(SLPM)	181.9	182
Propylene flow meter reading		
(FMR)	20	40
(SLPM)	99.3	198.6
Air flow meter reading		
(FMR)	35	50
(SLPM)	150.8	215.5
Spray distance		
(mm)	150	300
Powder feed rate		
(g/min)	15	45

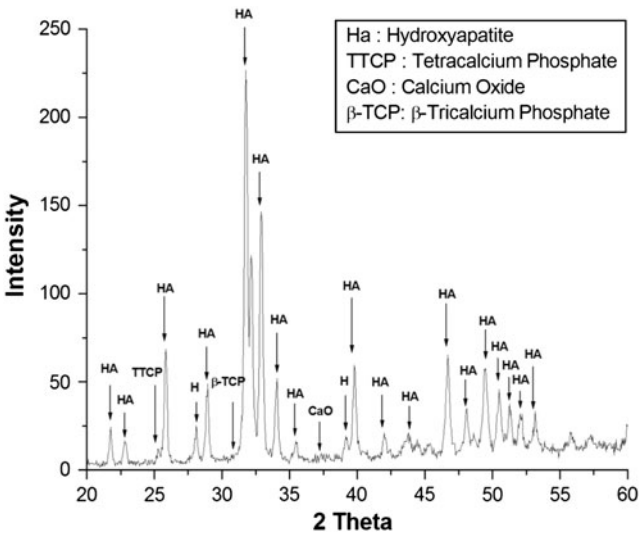

Fig. 3 Sample 24 XRD pattern

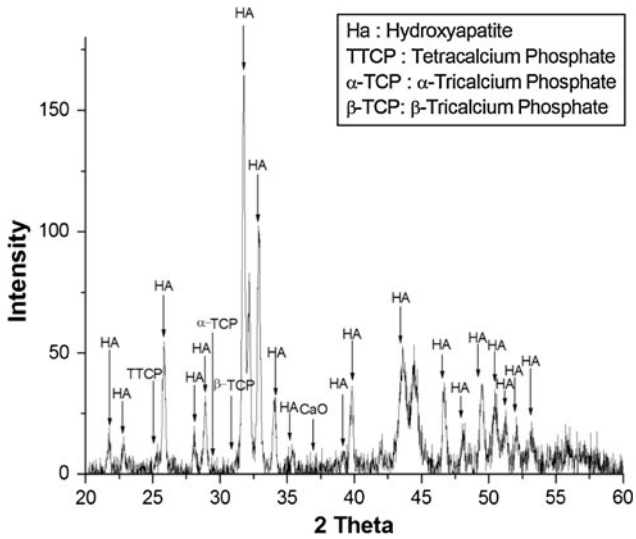

Fig. 4 Sample 29 XRD pattern

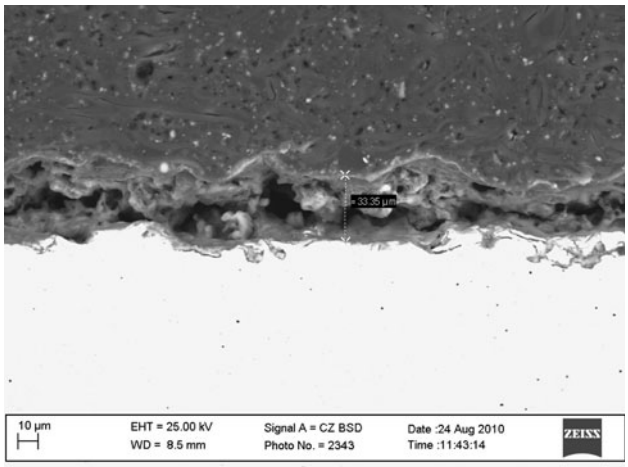

Fig. 5 Cross section of sample 24

Table 3 Crystallinity and purity results

Sample	Oxygen, FMR	Propylene, FMR	Air, FMR	Spray distance, mm	Powder feed rate, g/min	Crystallinity, %	Purity, %
1	30	20	35	150	15	90.28	99.80
2	45	20	35	150	15	86.66	99.61
3	30	40	35	150	15	88.6	99.67
4	45	40	35	150	15	87.96	99.32
5	30	20	50	150	15	84.28	99.37
6	45	20	50	150	15	88.14	99.15
7	30	40	50	150	15	88.39	99.53
8	45	40	50	150	15	88.22	99.11
9	30	20	35	300	15	78.67	98.70
10	45	20	35	300	15	85.49	99.75
11	30	40	35	300	15	87.82	99.76
12	45	40	35	300	15	87.31	99.80
13	30	20	50	300	15	80.41	98.89
14	45	20	50	300	15	84.04	99.29
15	30	40	50	300	15	91.16	99.43
16	45	40	50	300	15	84.91	99.18
17	30	20	35	150	45	91.82	99.11
18	45	20	35	150	45	89.05	99.76
19	30	40	35	150	45	88.69	99.71
20	45	40	35	150	45	91.67	99.65
21	30	20	50	150	45	89.61	99.84
22	45	20	50	150	45	86.52	97.56
23	30	40	50	150	45	86.65	99.26
24	**45**	**40**	**50**	**150**	**45**	**93.81**	**99.09**
25	30	20	35	300	45	85.63	98.60
26	45	20	35	300	45	84.29	99.00
27	30	40	35	300	45	90.17	99.49
28	45	40	35	300	45	83	98.58
29	**30**	**20**	**50**	**300**	**45**	**74.94**	**99.11**
30	45	20	50	300	45	84.19	99.52
31	30	40	50	300	45	84.36	99.58
32	45	40	50	300	45	83.44	99.71

Table 4 ANOVA table for the crystallinity model

Source	Sum of squares	Mean square	*F* value	*p* value Prob > *F*	Significance
Model significance	311.25	77.81	12.40	<0.0001	Significant
B-propylene flow rate	55.49	55.49	8.84	0.0061	
D-spray distance	155.41	155.41	24.76	<0.0001	
ABD	72.48	72.48	11.55	0.0021	
ACDE	27.86	27.86	4.44	0.0445	
Residual	169.45	6.28			
Cor total	480.70				
R^2	0.6475				
Adj R^2	0.5953				
Pred R^2	0.5048				
Adeq precision	12.035				

The highest purity was found to be 99.89%, and the lowest purity was found to be 97.56%, which met the >95% purity stipulated as outlined in the ASTM standard ISO 13779-1:2000 (Ref 38). The crystallinity and purity results for all the samples are presented in Table 3. As purity was acceptable for all the samples chosen (as >95%); thus, the crystallinity variation was seen as more important point to merit discussion. Levingstone (Ref 2) optimized the plasma spraying process for HA deposition and found a set of parameters which produce a coating of 87.6% crystallinity and 99.4% purity. Hence, the HVOF system has already proven as a novel method for HA deposition with maximum crystallinity and purity values of 93.81 and 99.84%, respectively.

4.2 Optimized Crystallinity

A schematic diagram of the setup of sample 24 (Table 4) is given in Fig. 6, which shows the flame size when compressed air, oxygen, propylene, and powder feed rate were set high. T_L represents low temperature when compressed air is high, and T_H represents high temperature

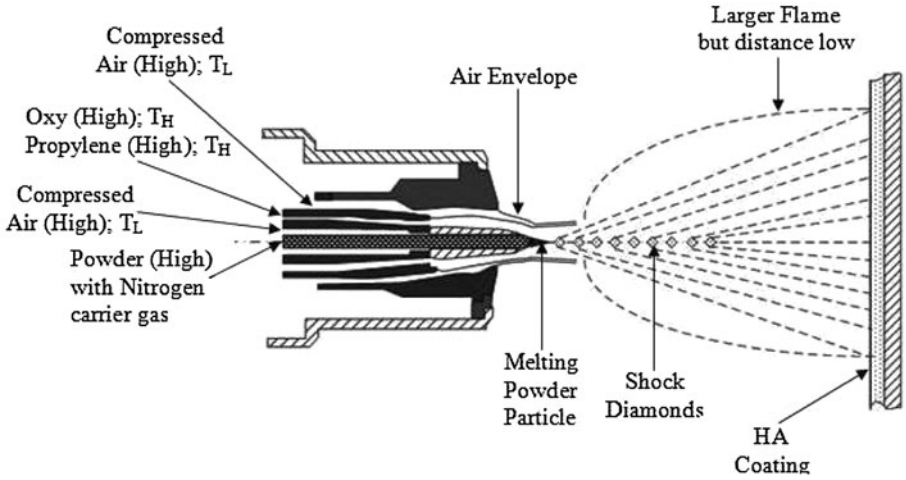

Fig. 6 Process regime for sample 24

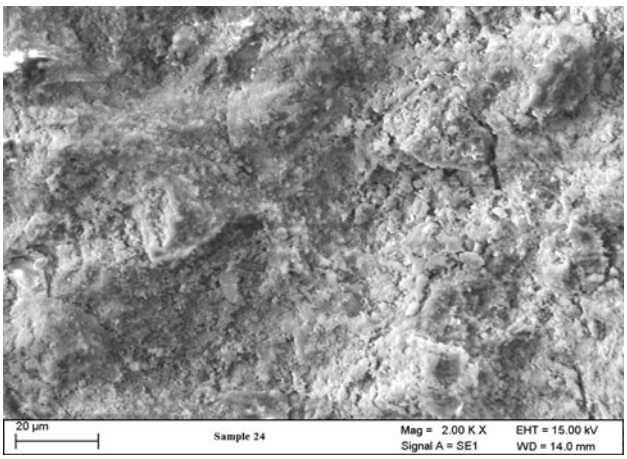

Fig. 7 SEM micrograph of sample 24 with maximum crystallinity

formed by fully molten particles, and the flame in contact with the sample surface resulting in the melting of the applied particles.

4.3 Crystallinity Model

The ANOVA table and model statistics for crystallinity model are shown in Table 4. The ANOVA table shows that the F value of the model was 12.40, which implies that the model was significant at a confidence level of 99%. The adjusted R^2 was found to be 0.5953, and predicted R^2 to be 0.5048, and the difference between these two was 0.0905 which was less than 0.2; these results indicate that the model adequately fits the experimental data and that the model was statistically acceptable.

It is clear from Table 4 that the spray distance (D) had the greatest effect on coating crystallinity. Adequate precision was found to be 12.035 which is greater than 4, indicating an adequate signal. The final mathematical model for crystallinity is given in Eq 3 in terms of actual factor.

$$\begin{aligned}\text{Crystallinity} = {} & +86.57 + 1.32 * B(\text{Propylene flow meter reading}) \\ & - 2.20 * D(\text{Spray distance}) \\ & - 1.51 * A * B * D(\text{Oxygen flow meter reading} * \text{Propylene flow meter reading} * \text{Spray distance})\end{aligned} \quad \text{(Eq 3)}$$

when both oxygen and propylene flow rate are high. Here, the hypothesis was that low crystallinity- and phase-loss occured because the dwell time of the powder was short and the powder feed rate was high. The flame was hotter and larger over the substrate, thereby recrystallizing the coating. Therefore, high crystallinity and purity would be expected at these parametric settings as they prove to be optimal in terms of maintaining crystallinity and purity levels compared to original powder.

The morphology of sample 24 which was coated by HA powder by the HVOF is shown in Fig. 7. This flame effect can thus be seen supporting the latter statement where a flattened surface was observed. This flattened surface was

As spray distance had the greatest effect (coded equation gave it a level of 2.20) but a negative effect, it suggests that spray distance should be kept low to yield high crystallinity. This makes sense with the previous discussion as this allows the flame to have a larger affect on the recrystallization effect of the coating.

The model shows Oxygen (A), Propylene (B) flow rate, and spray distance (D) as the next most influencing negative interactive factors ($A * B * D$). Again, this agrees with the previous statement that Oxygen and Propylene must be stoichiomatically balanced. Therefore, their effects must be aligned. However, it suggests keeping all these parameters low (negative effect −1.51) to get

high crystallinity. On the other hand, the third biggest effect is propylene flow rate (+1.32). Therefore, it should be kept high in this case. The reason for the contradiction is the large effect that spray distance (+2.2 versus −1.51) has on the ABD result. Therefore, preference must be given to the spray distance (D). These results support the effects of parameters used in DJ HVOF spraying of ceramics (Ref 31).

meter reading * Propylene flow meter reading * Air flow meter reading (ABC), Oxygen flow meter reading * Propylene flow meter reading * Spray distance, Air flow meter reading * Spray distance * Powder feed rate (CDE), Oxygen flow meter reading * Air flow meter reading * Spray distance * Powder feed rate (ACDE) were significant model terms. The final mathematical model for purity is given in Eq 4 in terms of coded factors.

$$\begin{aligned}\text{Purity} = {} & +99.31 + 0.12 * B(\text{Oxygen flow meter reading}) \\ & + 0.13 * A * D(\text{Oxygen flow meter reading} * \text{Spray distance}) \\ & + 0.15 * C * D(\text{Air flow meter reading} * \text{Spray distance}) \\ & + 0.13 * A * B * C(\text{Oxygen flow meter reading} * \text{Propylene flow meter reading} * \text{Air flow meter reading}) \\ & - 0.13 * A * B * D(\text{Oxygen flow meter reading} * \text{Propylene flow meter reading} * \text{Spray distance}) \\ & + 0.15 * C * D * E(\text{Air flow meter reading} * \text{Spray distance} * \text{Powder feed rate}) \\ & + 0.15 * A * C * D * E(\text{Oxygen flow meter reading} * \text{Air flow meter reading} * \text{Spray distance} * \text{Powder feed rate})\end{aligned} \quad \text{(Eq 4)}$$

4.4 Purity Model

The ANOVA table and model statistics for purity model are given in Table 5. The ANOVA table shows that the model F value was 5.13, which implies that the model was significant. The adjusted R^2 was found to be 0.4828 and predicted R^2 to be 0.2882, and the difference between this two is 0.1946, which is less than 0.2, indicating that the model adequately fits the experimental data. The R^2 results were low, however; but as the range of purity results from maximum to minimum was very close, the model would be deemed sensitive.

It is clear from the table that the effects of oxygen flow rate (A), air flow rate (C), spray distance (D), and powder feed rate (E) have the greatest effects on coating purity. Adequate precision was found to be 9.630 which was greater than 4, indicating an adequate signal. Values of "Prob $>$ F" less than 0.0500 indicated that the model terms were significant. In this case, interactions Oxygen flow meter reading * Spray distance (AD), Air flow meter reading * Spray distance (CD), Oxygen flow

One can see that each factor within an interaction was almost equally rated (0.15-0.12) although sometimes with positive or negative effect. However, all the parameters had similar effect in agreement with crystallinity effects. Thus, comparing with the coded equation for crystallinity where multipliers of 2.20 and so on were involved, this shows that these factors had more influence on crystallinity than (0.15) on purity.

4.5 Optimization

The optimized solution using the desirability function (maximum crystallinity and purity) as found by Design Expert is shown in Table 6. An oxygen flow meter reading of 45 FMR, propylene flow meter reading of 40 FMR, air flow meter reading of 35 FMR, spray distance of 150 mm, and powder feed rate of 45 g/min, yielding the models prediction of maximum crystallinity and purity, which were basically the conditions for sample 20 (Table 3). All of these parameters were the same as those used in sample 24 except for the air flow meter reading, experimentally

Table 5 ANOVA table for the purity model

Source	Sum of squares	Mean square	F value	p value Prob $>$ F	Significance
Model	4.31	0.62	5.13	0.0011	Significant
B-propylene flow rate	0.45	0.45	3.78	0.0636	
AD	0.58	0.58	4.84	0.0377	
CD	0.71	0.71	5.88	0.0232	
ABC	0.54	0.54	4.53	0.0437	
ABD	0.58	0.58	4.80	0.0385	
CDE	0.69	0.69	5.78	0.0243	
ACDE	0.76	0.76	6.33	0.0189	
Residual	2.88	0.12			
Cor total	7.19				
R^2	0.5996				
Adj R^2	0.4828				
Pred R^2	0.2882				
Adeq precision	9.630				

Table 6 Optimized spray parameters for HVOF sprayed HA

Sample	Optimized
Oxygen, FMR	45
Propylene, FMR	40
Air, FMR	35(a)
Spray distance, mm	150
Powder feed rate, g/min	45
Crystallinity, %	**92.53**(a)
Purity, %	**99.88**(a)

(a) Parameters/results which differ from sample 24

selected at 50 FMR. However, a comparison of the experimental results between samples 20 and 24 showed that sample 24 had the higher crystallinity, and the model predicted an optimized crystallinity of 92.53% and purity of 99.88%. Therefore, the model has tried to maximize purity also, but as the purity values are extremely high for most samples, the lower optimized crystallinity has suffered in its prediction. The sample 24 produced the highest crystallinity result of 93.81% but only slightly lower purity of 99.09%; thus, the model's optimized solution was deemed not as good as sample 24 in terms of crystallinity, yet having higher purity. The conclusion is that the parameters chosen for sample 24 are deemed as the optimized research parameters for HVOF spraying of HA.

5. Conclusions

In this current research, investigations to optimize the parameters for High Velocity Oxy-Fuel thermal-sprayed hydroxyapatite coatings were carried out to obtain higher crystallinity and purity. Coating crystallinity was found to be maximum (sample 24) when oxygen flow meter reading was selected at 45 FMR, propylene flow meter reading was selected at 40 FMR, air flow meter reading was selected at 50 FMR, spray distance was selected to 150 mm, and powder feed rate was selected to 45 g/min, which were almost the same as the DOE optimized solution. Therefore, the verification of experimental results showed that they did not contradict those of optimization. Coating purity was also found to be higher for the same parameters as those used in sample 24. According to DOE optimization solution, if the air flow meter reading was set low, then higher purity could be achieved; but the crystallinity would be lower in that case. Hence, in accordance with FDA stipulations, sample 24 already achieved >95% purity. Compared to plasma spray, the HVOF system has proven to be a novel method for HA deposition with maximum crystallinity and purity values of 93.81 and 99.84%, respectively, as only 87.6 and 99.4% crystallinity and purity values, respectively, were found when using FDA-approved plasma spray technique (2). Hence, although the primary aim of this research has been achieved, other properties like bond strength, roughness, porosity, hardness, and cell culture (osseointegration) must be assessed.

References

1. J. Stokes and L. Looney, Residual Stress in HVOF Thermally Sprayed Thick Deposits, *J. Surf. Coat. Technol.*, 2004, **177-178**, p 18-23
2. T.J. Levingstone, "Optimisation of Plasma Sprayed Hydroxyapatite Coatings," Ph.D. thesis, Dublin City University, Ireland, 2008, http://doras.dcu.ie/579/
3. P. Fauchais, Understanding Plasma Spraying, *J. Phys. D Appl. Phys.*, 2004, **37**, p R86
4. H.C. Gledhill, I.G. Turner, and C. Doyle, In Vitro Dissolution Behaviour of Two Morphologically Different Thermally Sprayed Hydroxyapatite Coatings, *Biomaterials*, 2001, **22**, p 695-700
5. H.C. Gledhill, I.G. Turner, and C. Doyle, In Vitro Fatigue Behaviour of Vacuum Plasma, Detonation Gun Sprayed Hydroxyapatite Coatings, *Biomaterials*, 2001, **22**, p 1233-1240
6. H.C. Gledhill, I.G. Turner, and C. Doyle, Direct Morphological Comparison of Vacuum Plasma Sprayed, Detonation Gun Sprayed Hydroxyapatite Coatings for Orthopaedic Applications, *Biomaterials*, 1999, **20**, p 315-322
7. T.J. Levingstone, *Ceramics for Medical Applications*, Dublin City University, Ireland, 2008, ISBN: 1-87232-752-4
8. S.J. Schneider, Jr., *Ceramics and Glasses*, Vol 4, ASM International, Ohio, USA, 1991, ISBN 13: 978-0-87170-282-1
9. P. Ducheyne, J. Beight, J. Cuckler, B. Evans, and S. Radin, Effect of Calcium Phosphate Coating Characteristics on Early Post-Operative Bone Tissue Ingrowth, *Biomaterials*, 1990, **11**, p 531-540
10. K. Soballe, The role of H-A-C in ingrowth prostheses, *Hydroxyapatite Ceramic, a Decade of Experience in Hip Arthroplasty, the Proceedings of a Two Day Symposium*, R. Furlong, Ed., Held at the Royal College of Surgeons of England on Thursday 2nd & Friday 3rd November 1995, Furlong Research Foundation, London, 1996, p 57-67
11. ASTM F1185-03, *Standard Specification for Composition of Ceramic Hydroxyapatite for Surgical Implants*, ASTM F1185-03, ASTM International, 2003
12. K.A. Gross, K. Heeman, and K.S. Saber-Samandari, Evaluation of Commercial Implants with Nanoindentation Defines Future Development Needs for Hydroxyapatite Coatings, *J. Biomed. Mater. Res.: Appl. Biomater.*, 2010, **93B**(1), p 1-8
13. Anonymous, Implants for Surgery-Hydroxyapatite. Part 2: Coatings of Hydroxyapatite, BS ISO 13779-2:2000, 2000
14. Y.C. Tsui, C. Doyle, and T.W. Clyne, Plasma Sprayed Hydroxyapatite Coatings on Titanium Substrates Part 2: Optimisation of Coating Properties, *Biomaterials*, 1998, **19**(11), p 2031-2043
15. L. Sun, C.C. Berndt, and C.P. Grey, Phase, Structural, Microstructural Investigations of Plasma Sprayed Hydroxyapatite Coatings, *Mater. Sci. Eng. A*, 2003, **360**(11/15), p 70-84
16. M.F. Morks and A. Kobayashi, Effect of Gun Current on the Microstructure, Crystallinity of Plasma Sprayed Hydroxyapatite Coatings, *Appl. Surf. Sci.*, 2007, **253**(17), p 7136-7142
17. M.P. Taylor, "Assessment of Plasma-Sprayed Hydroxyapatite Coatings," Ph.D. thesis, University of Birmingham, Birmingham, 1994
18. P. Cheang and K.A. Khor, Thermal Spraying of Hydroxyapatite (HA) Coatings: Effects of Powder Feedstock, *J. Mater. Process. Technol.*, 1995, **48**, p 429-436
19. C.H. Quek, K.A. Khor, and P. Cheang, Influence of Processing Parameters in the Plasma Spraying of Hydroxyapatite/Ti-6Al-4V Composite Coatings, *J. Mater. Process. Technol.*, 1999, **89-90**, p 550-555
20. Y.P. Lu, S.T. Li, R.F. Zhu, and M.S. Li, Further Studies on the Effect of Stand-off Distance on Characteristics of Plasma Sprayed Hydroxyapatite Coating, *Surf. Coat. Technol.*, 2002, **157**, p 221-225
21. J.F. Li, H. Liao, B. Normand, C. Cordier, G. Maurin, J. Foct, and C. Coddet, Uniform Design Method for Optimization of Process Parameters of Plasma Sprayed TiN Coatings, *Surf. Coat. Technol.*, 2003, **176**, p 1-13
22. T.J. Steeper, D.J. Varacalle, Jr., G.C. Wilson, W.L. Riggs, A.J. Rotolico, and J.E. Nerz, A Design of Experiment Study of Plasma Sprayed Alumina-Titania Coatings, *Thermal Spray:*

International Advances in Coatings Technology, 13th International Thermal Spray Conference, C.C. Berndt, Ed., 28th May-5th June, 1992, Orlando, FL, 1992
23. T.J. Steeper, D.J. Varacalle, Jr., G.C. Wilson, W.L. Riggs, A.J. Rotolico, and J.E. Nerz, Optimizing Plasma Spraying Alumina-Titania Coatings Using Statistical Methods, *Thermal Spray Coatings: Research, Design and Applications*, *5th National Thermal Spray Conference*, C.C. Berndt and T.F. Bernecki, Ed., June 7-11, 1993, Anaheim, CA, 1993
24. J.R. Mawdsley, Y.J. Su, K.T. Faber, and T.F. Bernecki, Optimization of Small-Particle Plasma-Sprayed Alumina Coatings Using Designed Experiments, *Mater. Sci. Eng. A*, 2001, **308**, p 189-199
25. T.J. Steeper, D.J. Varacalle, Jr., G.C. Wilson, W.L. Riggs, A.J. Rotolico, and J.E. Nerz, A Taguchi Design of Experiment Study of Plasma Sprayed Alumina Coatings, *Thermal Spray Coatings: Research, Design and Applications*, 1993
26. D.F. Gibbons and K.A. Buran, *Microscopic Analysis of Retrieved Polymethylmethacrylate (PMMA) Bone Cement, Implant Retrieval: Material and Biological Analysis*, National Bureau of Standards Special Publication 601, National Bureau of Standards, Washington, DC, 1981
27. B. Lin, M. Jean, and J. Chou, Using Response Surface Methodology for Optimizing Deposited Partially Stabilized Zirconia in Plasma Spraying, *Appl. Surf. Sci.*, 2007, **253**(6), p 3254-3262
28. J. Cizek, K.A. Khor, and Z. Prochazka, Influence of Spraying Conditions on Thermal and Velocity Properties of Plasma Sprayed Hydroxyapatite, *Mater. Sci. Eng. C*, 2007, **27**(2), p 340-344
29. S. Dyshlovenko, C. Pierlot, L. Pawlowski, R. Tomaszek, and P. Chagnon, Experimental Design of Plasma Spraying and Laser Treatment of Hydroxyapatite Coatings, *Surf. Coat. Technol.*, 2006, **201**, p 2054-2060
30. S. Dyshlovenko, L. Pawlowski, P. Roussel, D. Murano, and A. Le Maguer, Relationship Between Plasma Spray Operational Parameters and Microstructure of Hydroxyapatite Coatings and Powder Particles Sprayed into Water, *Surf. Coat. Technol.*, 2006, **200**(12-13), p 3845-3855
31. J. Stokes, *Theory and Application of Sulzer Metco High Velocity Oxy-Fuel (HVOF) Thermal Spray Process*, © Dublin City University, 2008, ISBN 1-87232-753-2, ISSN 1649-8232
32. S.W.K. Kweh, K.A. Khor, and P. Cheang, Plasma-Sprayed Hydroxyapatite (HA) Coatings with Flame-Spheroidized Feedstock: Microstructure and Mechanical Properties, *Biomaterials*, 2000, **21**, p 1223-1234
33. J. Stokes and L. Looney, HVOF System Definition to Maximise the Thickness of Formed Components, *J. Surf. Coat. Technol.*, 2001, **148**(1), p 18-24
34. F.W. Munjone and G. Irons, The Evolution of Thermal Spray Automation, *Proceedings of the 5th National Thermal Spraying Conference*, Anaheim, CA, USA, 1993, p 263-273
35. G. Irons, Thermal Spray Applications Speeds, *Proceedings of the 14th International Thermal Spray Conference*, Kobe, Japan, 1995, p 1165-1168
36. K.A. Gross, C.C. Berndt, and V.J. Iacono, Variability of Hydroxyapatite Coated Dental Implants, *Int. J. Oral Maxillofac. Implants*, 1998, **13**, p 601-610
37. K.A. Gross, C.C. Berndt, and H. Herman, Formation of the Amorphous Phase in Hydroxyapatite Coatings, *J. Biomed. Mater. Res.*, 1998, **39**, p 407-414
38. BS ISO13779, *Implants for Surgery-Hydroxyapatite. Part 1: Ceramic Hydroxyapatite*, BS ISO 13779-1:2000, International Organisation for Standards, USA, 2000